J. Fac. Pharm. Ankara / Ankara Ecz. Fak. Derg., 49(4): 1067-1078, 2025
Doi: 10.33483/jfpau.1760832

ORIGINAL ARTICLE / ÖZGÜN MAKALE

QUINOXALINE DERIVATIVES AS α-GLUCOSIDASE INHIBITORS: SYNTHESIS AND BIOLOGICAL EVALUATION

ALFA-GLUKOZİDAZ İNHİBİTÖRLERİ OLARAK KİNOKSALİN TÜREVLERİ: SENTEZ VE BİYOLOJİK DEĞERLENDİRME

Merve ARI[1], Zeynep SOYER[1]*

[1]Ege University, Faculty of Pharmacy, Department of Pharmaceutical Chemistry, 35100, İzmir, Türkiye

ABSTRACT

Objective: *The primary aim of this study is to develop novel α-glucosidase inhibitors with high efficacy through rational design and synthesis strategies utilizing pharmacophoric scaffolds previously defined in the literature. This research aims to contribute to the discovery of clinically relevant potential drug candidates for the treatment of diabetes mellitus. Towards this end, some quinoxaline-hydrazone derivatives were synthetized, and their α-glucosidase inhibition were experimentally investigated. Furthermore, to elucidate the enzyme inhibition mechanism and the ligand-enzyme interactions at the molecular level, molecular docking studies and enzyme inhibition kinetic analyses were conducted on the most active compound.*

Material and Method: *The quinoxaline-hydrazone derivatives were synthesized via a three-step procedure. The structures of the synthesized compounds were confirmed by spectral analysis, including FT-IR, ^{1}H NMR, ^{13}C NMR and HR-MS techniques. The α-glucosidase inhibition and enzyme kinetic study were conducted in vitro with a standard colorimetric assay, using p-nitrophenyl-α-D-glucopyranoside (pNPG) as the substrate. Acarbose was used as a reference standard. Inhibiton % and the IC_{50} values were calculated to assess the inhibitory potency of the compounds. Molecular docking study was executed by the GOLD 5.2 program.*

Result and Discussion: *The biological activity assessment showed that the synthesized quinoxaline-hydrazone derivatives exhibited inhibitory activity with varying percentages against the α-glucosidase. Among the compounds tested, 2 bearing p-hydroxy subtituent on the N-phenyl ring is the most effective compound and displayed a stronger α-glucosidase inhibitory activity with IC_{50} value of 0.413 ± 0.048 mM compared to the standard drug acarbose ($IC_{50}=1.211 \pm 0.08$ mM). Furthermore, the kinetic study showed that the most active compound 2 acted as a competitive inhibitor of the α-glucosidase enzyme, with a K_i value of 115.6 µM. Additionally, molecular docking analysis showed that the molecular interactions between compound 2 and the enzyme's active site, and these interactions were observed to be consistent with the biological activity and kinetic results. These findings suggest that the quinoxaline-hydrazone scaffold could serve as a promising lead structure for the development of novel potent antidiabetic agents.*

Keywords: *Diabetes, hydrazone, quinoxaline, synthesis, α-glucosidase inhibitors*

* **Corresponding Author / Sorumlu Yazar:** Zeynep Soyer
e-mail / e-posta: zeynep.soyer@ege.edu.tr, **Phone / Tel.:** +905335217037

Submitted / Gönderilme : 09.08.2025
Accepted / Kabul : 17.11.2025
Published / Yayınlanma : 31.12.2025

Presented at the 14th International Symposium on Pharmaceutical Sciences (ISOPS-14), 25-28 June 2024, Ankara, Turkey.

ÖZ

Amaç: *Bu çalışmanın temel amacı, literatürde daha önce tanımlanmış farmakoforik yapılardan faydalanarak, rasyonel tasarım ve sentez stratejileri yoluyla yüksek inhibitör potansiyeline sahip yeni α-glukozidaz inhibitörleri geliştirmektir. Bu araştırma, diabetes mellitus tedavisinde klinik öneme sahip potansiyel ilaç adaylarının keşfine yönelik bilimsel katkı sağlamayı hedeflemektedir. Bu kapsamda, çalışmamızda çeşitli kinoksalin-hidrazon türevleri sentezlenmiş ve bu bileşiklerin α-glukozidaz inhibitör etkinlikleri deneysel olarak incelenmiştir. Ayrıca, enzim inhibisyon mekanizmasının ve ligand-enzim etkileşimlerinin moleküler düzeyde aydınlatılması amacıyla, en yüksek aktiviteye sahip bileşik üzerinde moleküler doking çalışmaları ve enzim inhibisyon kinetik analizleri gerçekleştirilmiştir.*

Gereç ve Yöntem: *Kinoksalin-hidrazon türevleri, üç basamaklı bir sentez protokolü ile elde edilmiştir. Sentezlenen bileşiklerin yapısal karakterizasyonu, FT-IR, ^{1}H NMR, ^{13}C NMR ve HR-MS tekniklerini içeren spektral analiz yöntemleriyle doğrulanmıştır. α-Glukozidaz inhibitör aktivite ve enzim inhibisyon kinetiği çalışmaları, in vitro koşullarda p-nitrofenil-α-D-glukopiranozid (pNPG) substratı kullanılarak standart bir kolorimetrik yöntemle değerlendirilmiştir. Kontrol maddesi olarak akarboz kullanılmıştır. Bileşiklerin inhibitör etkinliklerinin belirlenmesi amacıyla % inhibisyon ve IC_{50} değerleri hesaplanmıştır. Moleküler doking çalışması, GOLD 5.2 programı kullanılarak gerçekleştirilmiştir.*

Sonuç ve Tartışma: *Biyolojik aktivite değerlendirmeleri, sentezlenen kinoksalin-hidrazon türevlerinin α-glukozidaz enzimine karşı değişen oranlarda inhibitör aktivite sergilediğini göstermiştir. Test edilen bileşikler arasında, N-fenil halkasında para-hidroksi substitüenti taşıyan bileşik 2 en aktif bileşik olup, standart ilaç akarboza (IC_{50} = 1.211 ± 0.08 mM) kıyasla daha güçlü bir α-glukozidaz inhibitör aktivitesi (IC_{50} = 0.413 ± 0.048 mM) göstermiştir. Bunun yanı sıra, enzim inhibisyon kinetiği çalışması, en aktif bileşik 2'nin 115.6 μM'lik bir K_i değeri ile α-glukozidaz enzimini kompetitif inhibitör mekanizmasıyla engellediğini ortaya koymuştur. Ayrıca, moleküler doking analizi, bileşik 2 ile enzimin aktif bölgesi arasındaki moleküler etkileşimleri aydınlatmış ve bu etkileşimlerin biyolojik aktivite ile kinetik sonuçlarla tutarlı olduğu gözlemlenmiştir. Bu bulgular, kinoksalin-hidrazon iskeletinin, yeni ve potansiyel antidiyabetik ajanların geliştirilmesinde umut verici bir lider yapı olabileceğini düşündürmektedir.*

Anahtar Kelimeler: *Diyabet, hidrazon, kinoksalin, sentez, α-glukozidaz inhibitörleri*

INTRODUCTION

Diabetes mellitus represents one of the most significant global health challenges today. The rising prevalence is attributed to poor nutrition, insufficient physical activity, and obesity, with increasing diagnoses reported worldwide [1,2]. The International Diabetes Federation (IDF) stated that 4.2 million deaths globally in 2019 resulted from hyperglycemia-related complications. Projections indicate that by 2045, diabetes will affect over 700 million people, comprising approximately 25% of the world's population [3]. This chronic metabolic disorder arises from either inadequate insulin production or impaired insulin efficacy. Diabetes is clinically classified into three major types: type 1, defined with insulin defect; type 2, associated with insulin resistance and dysfunctional insulin utilization despite adequate secretion; and gestational diabetes. Notably, type 2 diabetes accounts for 87-91% of cases, while type 1 represents 7-12% [2]. Uncontrolled diabetes leads to severe complications, including nephropathy, neuropathy, cardiovascular damage, and retinopathy [4,5]. Postprandial hyperglycemia is recognized as a primary risk factor in diabetes pathogenesis and progression [6], with evidence demonstrating that effective postprandial glucose management can delay type 2 diabetes onset in prediabetic individuals [7].

Current therapeutic guidelines recommend metformin, sulfonylureas, α-glucosidase inhibitors (AGIs), and dipeptidyl peptidase 4 (DPP-4) inhibitors as first-line treatments for type 2 diabetes [8]. Among these, AGIs effectively regulate postprandial glycemia by delaying intestinal carbohydrate digestion [9]. Unabsorbed carbohydrates undergo bacterial fermentation in the ileum, enhancing gut microbiota diversity and contributing to reduced inflammation and increased longevity [10]. Clinically established AGIs include acarbose, voglibose, and miglitol (Figure 1). However, their sugar-derived structures limit therapeutic efficacy, and prolonged use frequently causes gastrointestinal adverse effects such as diarrhea, bloating, and abdominal pain, with incidence correlating to dosage and treatment

duration. Additionally, emerging evidence suggests potential development of acarbose resistance over time [11]. These limitations underscore the critical need for novel inhibitor development to expand therapeutic options.

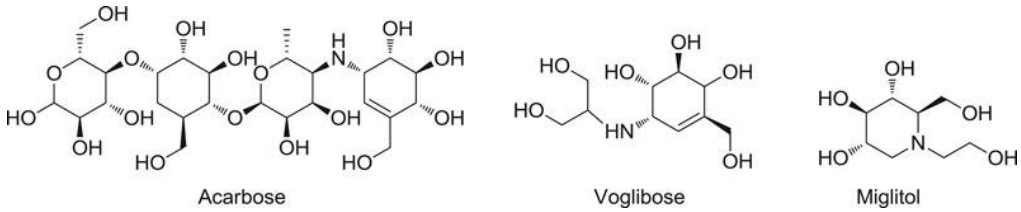

Figure 1. The chemical structures of clinically used AGIs

In drug discovery, heterocyclic scaffolds are strategically employed to enhance solubility, metabolic stability, and hydrogen-bonding capacity of bioactive compounds. Over 85% of biologically active molecules contain at least one heterocyclic moiety, highlighting their indispensable role in modern medicinal chemistry [12]. The quinoxaline scaffold, in particular, features prominently in pharmacologically active agents, including antidiabetic compounds [13-16]. Similarly, the hydrazone functional group exhibits well-documented biological significance across antitumor, antimicrobial, and antidiabetic domains, attributed to its capacity for forming stable chelates and hydrogen bonds with biological targets [17,18].

Given the promising pharmacological profiles of both quinoxaline and hydrazone moieties, we designed and synthesized some quinoxaline-hydrazone derivatives as potential α-glucosidase inhibitors for diabetes management. To elucidate selected most active compound's mechanism of action, enzyme kinetic studies and molecular docking analyses were conducted to characterize the inhibitory mechanism and molecular interactions with α-glucosidase enzyme.

MATERIAL AND METHOD

Chemistry

All reagents used in the synthesis were purchased from Sigma, Merck, and Fluka, and employed without further purification. Melting points were determined using a Stuart SMP30 apparatus. Infrared spectra were recorded in attenuated total reflectance (ATR) mode using a PerkinElmer Spectrum 100 FT-IR spectrophotometer. Proton (^{1}H) and carbon (^{13}C) NMR spectra were acquired on a Bruker Avance III HD 600 MHz instrument. High-resolution mass spectra (HR-MS) were obtained using an Agilent 1260 Infinity HPLC system coupled with an Agilent 6550 iFunnel Accurate-Mass QTOF-MS (Agilent Technologies, Santa Clara, CA, USA). Coupling constants (*J*) are reported in Hertz (Hz), and chemical shifts are expressed as δ values in parts per million (ppm), relative to tetramethylsilane (TMS, δ 0.00, singlet). Signal multiplicities are denoted as singlet (s), doublet (d), and multiplet (m).

The intermediates quinoxaline-2,3(1*H*,4*H*)-dione (1a), 3-hydrazinoquinoxalin-2-(*1H*)-one (1b) and, the final compounds were synthesized in accordance with procedures reported in the literatures.

Synthesis of Quinoxaline-2,3(1*H*,4*H*)-dione (1a)

A mixture of *o*-phenylenediamine (0.02 mol), oxalic acid dihydrate (0.03 mol), and 4 N HCl (17 ml) was refluxed for 1 h. Upon completion, the reaction was cooled to ambient temperature. The precipitated solid was filtered, washed thoroughly with water, and dried under vacuum. Quinoxaline-2,3(1*H*,4*H*)-dione was obtained in pure form without requiring additional purification [19].

Synthesis of 3-Hydrazinoquinoxalin-2-(*1H*)-one (1b)

A mixture of quinoxaline-2,3(1*H*,4*H*)-dione (0.005 mol) and hydrazine hydrate (4 ml, 0.089 mol) in water (2 ml) was refluxed for 3 h. Upon completion, the reaction mixture was cooled to ambient

temperature, and the resulting precipitation was collected by filtration. The crude compound was recrystallized from ethanol to obtain pure 3-hydrazinoquinoxalin-2(1*H*)-one [20].

Synthesis of Final Compounds (1-5)

A condensation reaction was performed by refluxing equimolar quantities of 3-hydrazinoquinoxalin-2(1*H*)-one (0.24 mmol) and appropriate aldehydes (0.24 mmol) in absolute ethanol (40 ml). Reaction progress was controlled by thin-layer chromatography (TLC) until completion of reaction. After refrigerated to ambient temperature, the precipitated crude was obtained via filtration and subsequently purified by recrystallization from ethanol, affording the target quinoxaline-hydrazone derivatives [21].

3-[2-(phenylmethylidene)hydrazyl]quinoxaline-2-(1*H*)one (1)

Yellow solid. Mp: 240-242 ºC (245-247 ºC [39]). Yield 46%. IR $_{vmax}$ (FT/ATR): 3174 (N-H stretch), 3055, 3006 (Aromatic C-H stretch), 2889 (Aliphatic C-H stretch), 1690 (C=O stretch), 1670, 1611 (C=N stretch), 1562 (C=C stretch), 1209 (C-N stretch) cm^{-1}. ^{1}H NMR 600 MHz, DMSO-d_6: *δ* 12.43 (1H, s, NH-quinoxaline), 11.26 (1H, s, NH-hydrazone), 8.59 (1H, s, HC=N), 7.73 (2H, d, *J = 7.62 Hz*), 7.54 (1H, d, *J = 7.5 Hz*), 7.51-7.41 (3H, m), 7.25-7.18 (3H, m) ppm. ^{13}C NMR 600 MHz, DMSO-d_6: *δ* 151.31 (C=O), 147.16, 146.62, 135.26, 133.32, 130.09, 129.29 (x2C), 129.05, 127.34 (x2C), 126.00, 125.15, 123.97, 115.51 ppm. HRMS (ESI/Q-TOF) m/z: $[M+H]^+$ Calcd for $C_{15}H_{13}N_4O$ 265.1084; Found 265.1121. Mass Difference (ppm); 0.98.

3-[2-((4-hydroxyphenyl)methylidene)hydrazyl]quinoxaline-2-(1*H*)one (2)

Yellow solid. Mp: 297.8 ºC (285 ºC (decomp) [37]). Yield 67%. IR ν_{max} (FT/ATR): 3486 (O-H stretch), 3308 (N-H stretch), 3195 (Aromatic C-H stretch), 2995, 2890 (Aliphatic C-H stretch), 1682 (C=O stretch), 1622, 1605 (C=N stretch), 1588, 1571, 1513 (C=C stretch), 1272 (C-O stretch) cm^{-1}. ^{1}H NMR (400 MHz, DMSO-d_6): *δ* 10.96 (1H, s, NH-quinoxaline), 10.35 (1H, s, NH-hydrazone), 8.43 (1H, s HC=N), 7.54 (2H, d, *J = 8.0 Hz*, Phenyl), 7.48-7.43 (1H, m, Quinoxaline), 7.18-7.15 (3H, m, Quinoxaline), 6.82 (2H, d, *J = 8.0 Hz*, Phenyl) ppm. ^{13}C NMR (600 MHz, DMSO-d_6): δ 159.57 (C=O), 151.35, 147.68, 146.55, 133.53, 130.99, 129.12 (x2C), 126.24, 125.77, 124.76, 123.93, 116.18 (x2C), 115.46 ppm. HRMS (ESI/Q-TOF) m/z: $[M+H]^+$ Calcd for $C_{15}H_{13}N_4O_2$ 281.1033; Found 281.1097. Mass Difference (ppm); 1.79.

3-[2-((4-methoxyphenyl)methylidene)hydrazyl]quinoxaline-2-(1*H*)one (3)

Yellow solid. Mp: 246-249 ºC (240-244 ºC [39]). Yield 69%. 3218 (N-H stretch), 3058 (Aromatic C-H stretch), 2935, 2888, 2835 (Aliphatic C-H stretch), 1666 (C=O stretch), 1607 (C=N stretch), 1562, 1501 (C=C stretch), 1249 (C-O stretch) cm^{-1}. ^{1}H NMR 400 MHz, DMSO-d_6: *δ* 12.32 (1H, s, NH-quinoxaline), 11.04 (1H, s, NH-hydrazone), 8.49 (1H, s, HC=N), 7.65 (2H, d, *J= 7.8 Hz*, Phenyl), 7.50-7.44 (1H, m, Quinoxaline), 7.19-7.15 (2H, m, Quinoxaline), 7.04-6.94 (3H, m, Quinoxaline and Phenyl), 3.80 (3H, s, O-CH_3) ppm. ^{13}C NMR 600 MHz, DMSO-d_6: *δ* 161.02 (C=O), 151.35, 147.17, 146.56, 133.46, 129.09, 128.94 (x2C), 127.83, 125.85, 124.89, 123.93, 115.48, 114.79 (x2C), 55.76 (-OCH_3) ppm. HRMS (ESI/Q-TOF) m/z: $[M+H]^+$ Calcd for $C_{16}H_{15}N_4O_2$ 295.1190; Found 295.1228. Mass Difference (ppm); 1.12.

4-[[2-(3,4-Dihydro-3-oxo-2-quinoxalinyl)hydrazinylidene]methyl]benzoic acid (4)

Yellow solid. Mp: 315 ºC (decomp) (379-380 ºC [40]). Yield 81.6%. IR ν_{max} (FT/ATR): 3465 (O-H stretch), 3333 (N-H stretch), 3147, 3006 (Aromatic C-H stretch), 2908, 2857 (Aliphatic C-H stretch), 1695 (C=O stretch), 1650 (C=O stretch), 1621, 1611 (C=N stretch), 1566, 1508 (C=C stretch), 1244 (C-O stretch) cm^{-1}. ^{1}H NMR 600 MHz, DMSO-d_6: *δ* 12.47 (1H, s, NH-quinoxaline), 8.68 (1H, s, HC=N), 8.02 (2H, d, *J= 8 Hz*, Phenyl), 7.91 (2H, d, *J = 8 Hz*, Phenyl), 7.60 (1H, d, *J= 7.7 Hz*, Quinoxaline), 7.24-7.19 (3H, m, Quinoxaline) ppm. ^{13}C NMR 600 MHz, DMSO-d_6: *δ* 167.22 (C=O, carboxylic acid), 154.17 (C=O), 151.20, 145.88, 137.32, 133.55, 130.18, 129.22 (x2C), 127.97 (x2C), 126.75, 125.01, 124.58, 120.10, 116.46 ppm. HRMS (ESI/Q-TOF) m/z: $[M+H]^+$ Calcd for $C_{16}H_{13}N_4O_3$ 309.0982; Found 309.1008. Mass Difference (ppm); 0.80.

3-[2-((4-nitrophenyl)methylidene)hydrazyl]quinoxaline-2-(1*H*)one (5)

Yellow solid. Mp: 301.4 ºC. Yield 18%. IR ν_{max} (FT/ATR): 3523, 3374, 3296 (N-H stretch), 3111, 3011(Aromatic C-H stretch), 2890, 2815 (Aliphatic C-H stretch), 1675 (C=O stretch), 1644, 1614 (C=N stretch), 1564, 1531, 1508, 1494, 1473 (C=C stretch) 1340 (N=O stretch), 1210 (C-O stretch) cm^{-1}. ^1H NMR 600 MHz, DMSO-d_6: δ 12.50 (1H, s, NH-quinoxaline), 11.60 (1H, s, NH-hydrazone), 8.68 (1H, s CH=), 8.31 (2H, d, *J= 8 Hz*, Phenyl), 7.97 (2H, d, *J = 8.4 Hz*, Phenyl), 7.58 (1H, d, *J= 7.7 Hz*, Quinoxaline), 7.28-7.22 (3H, m, Quinoxaline) ppm. ^{13}C NMR 600 MHz, DMSO-d_6: δ 151.24 (C=O), 147.87, 147.58, 144.38, 141.65, 133.03, 129.46, 128.06 (x2C), 126.30, 125.74, 124.59 (x2C), 124.06, 115.60 ppm. HRMS (ESI/Q-TOF) m/z: $[M+H]^+$ Calcd for $C_{15}H_{12}N_5O_3$ 310.0935; Found 310.0933. Mass Difference (ppm); -0.06.

Biological Activity

The determination of α-glucosidase inhibition and the kinetic studies of the final compounds were conducted using identical equipment and materials. The α-glucosidase enzyme from *Saccharomyces cerevisiae* was obtained from Sigma Aldrich. The substrate, *p*-nitrophenyl-*α*-D-glucopyranoside (PNPG), was purchased from TCI, while the reference compound acarbose was acquired from Acros. Buffer pH measurements were performed using a Hanna pH meter, and spectrophotometric analyses were conducted with a Varioskan microplate reader (Thermo Scientific) utilizing 96-well microplates.

***α*-Glucosidase Inhibition Study**

Serial dilutions of the test compounds and acarbose were prepared in dimethyl sulfoxide (DMSO) and aliquoted into microplate wells containing the enzyme solution in phosphate buffer (pH 6.8). Following a 5-minute incubation at 37°C, the enzymatic reaction was initiated by adding the substrate solution (*p*-nitrophenyl-*α*-D-glucopyranoside, PNPG, in buffer). Absorbance was then monitored spectrophotometrically at 405 nm. All measureaments were performed in triplicate. DMSO served as the solvent control, while acarbose was employed as the positive control. Inhibition % values were calculated with GraphPad Prism 8. Inhibition percentages were placed versus inhibitory concentrations and IC_{50} value was calculated with nonlinear regression analysis (r^2>0.95) by GraphPad Prism 8 [22-25].

Enzyme Kinetic Study

To elucidate the inhibitory mechanism, solutions of the test compound (2) were prepared in DMSO at concentrations of I_{60}, I_{40}, and I_{20} μM. The substrate, *p*-nitrophenyl-*α*-D-glucopyranoside (PNPG), was dissolved in pH 6.8 phosphate buffer to yield final concentrations of 2.0, 1.0, 0.5, and 0.25 mM. Enzyme activity was measured spectrophotometrically at 405 nm using the established protocol described earlier [26,27]. For each substrate concentration, absorbance values were measured for both the uninhibited control and inhibitor-containing reactions, from which initial reaction velocities were calculated. Michaelis-Menten curves and Lineweaver-Burk plots were constructed by plotting reaction velocities against substrate concentrations using GraphPad Prism 8 software.

Molecular Docking Study

A homology model of *α*-glucosidase (*Saccharomyces cerevisiae)* was set up for structural analysis. The protein sequence (UniProtKB accession: P53341) was obtained from the UniProt database [28]. Template identification was performed using UCSF Chimera, with crystal structure 3A47 selected based on its high sequence identity (>72%) to the target protein. The target-template alignment was automated in UCSF Chimera, followed by model generation to produce five candidate structures. Model validation was conducted through stereochemical assessment using PROCHECK-Ramachandran plots, complemented by geometric quality evaluation with ERRAT and Verify3D. The model exhibiting optimal validation metrics was selected for subsequent molecular docking simulations. Docking was executed by the GOLD 5.2 docking program with default setup. Docking of the compounds was sphere around the compounds 25 Å around the backbone carbon of Phe311 residue, which is the amino acid in the active site, and 50 conformations were allowed [29-33].

RESULT AND DISCUSSION

Chemistry

In this study, some quinoxaline-hydrazone hybrid compounds were synthesized to examine their α-glucosidase inhibitory activities. The synthesis of the compounds is illustrated in Scheme 1.

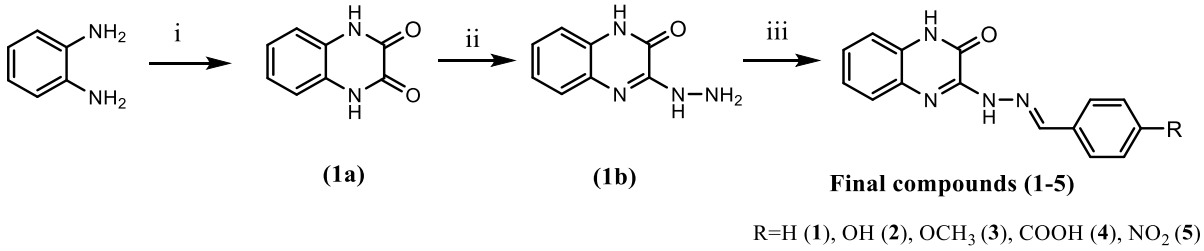

Scheme 1. The final compounds' synthesis scheme

As depicted in Scheme 1, the intented compounds were synthesized via a three-step sequence. Initially, quinoxaline-2,3(1*H*,4*H*)-dione was prepared through the reaction of oxalic acid with *o*-phenylenediamine in 4N HCl. Subsequently, this intermediate was treated with hydrazine hydrate in aqueous medium to yield 3-hydrazinoquinoxalin-2(1*H*)-one. Finally, condensation of 3-hydrazinoquinoxalin-2(1*H*)-one with suitable aldehydes afforded the target compounds. A comprehensive literature review revealed that none of the title compounds had been previously reported as α-glucosidase inhibitors. This study thus presents their first report as inhibitors of this enzyme. The compounds 1-4 are reported for their varied biological activities including antimicrobial activity (for compounds 1-3), anticancer activity (for compounds 2 and 4) [34-38,40]. Compound 5 is listed compound with Chemical Abstract Registry Number (CAS RN) 2981764-17-2, but corresponding scientific reference data are not available. The detailed synthetic procedure and spectral data for the title molecules are provided in the Material and Method section.

The chemical structures of the title compounds were confirmed by FT-IR, ^{1}H NMR, ^{13}C NMR, and HR-MS spectral analyses. With regard to IR data, the characteristic stretching absorbtion bands due to O-H, N-H, C=O and C=N groups were detected in the range of ν_{max}=3486-3465, 3523-3174, 1695-1666 and 1670-1605 cm^{-1}, respectively. Additional diagnostic absorption bands were observed in the spectra of final compounds.

The ^{1}H and ^{13}C NMR spectra exhibited resonances for aromatic and aliphatic protons/carbons within characteristic chemical shift ranges [22,23]. For instance, in the ^{1}H NMR spectra, diagnostic signals corresponding to the quinoxaline N-H and hydrazone N-H protons were observed as a singlet between at δ 12.50-10.96 and 11.60-10.35 ppm, respectively. The signals of azomethine (HC=N) protons appeared at δ 8.43-8.68 ppm, consistent with literature values [24]. In addition, the aromatic and aliphatic proton signals were detected in their expected regions and showed the predicted multiplicities, confirming the suggested structure. In the ^{13}C NMR spectra, the carbonyl carbons of the quinoxalinone nucleus resonate between δ 159.57-151.24 ppm, while the carbonyl carbon of the carboxylic acid was detected at 167.22 ppm for compound 4. Aromatic carbons appeared between δ 114.79 and 147.68 ppm, while the aliphatic methoxy carbon (-OCH_3) exhibited a signal at δ 55.76 ppm, consistent with its electron-donating substituent role. The structures and purities of the synthesized compounds were additionally confirmed by HR-MS analysis, as the observed m/z values of the molecular ion peaks were in excellent agreement with the corresponding calculated molecular weights.

Biological Activity

α-Glucosidase Inhibition Study

The *α*-glucosidase inhibitory potency of the compounds was evaluated spectrophotometrically using acarbose as a reference standard. Due to solubility limitations, the inhibition percentages for compounds 1, 3-5 are presented in Table 1 at their highest studied concentrations, while the IC_{50} value for compound 2 is shown in Table 2.

Table 1. The inhibitor effects of compounds 1, 3-5 and Acarbose against α-glucosidase enzyme

Compound	Inhibition% (0.2 mM)	Inhibition% (0.1 mM)	Inhibition% (0.025 mM)
1	24.77	9.36	4.36
3	26.28	18.14	NA
4	ND	32.45	11.20
5	ND	ND	18.01
Acarbose	20.38	14.79	6.53

NA=Not active at the concentration studied; ND=Not determined

Table 2. The α-glucosidase inhibitory activities of compound 2 and Acarbose *in vitro*

Compounds	IC_{50}±SEM(mM)[a]
2	0.413 ± 0.048
Acarbose	1.211 ± 0.08

[a]The data are means ± standard error of the triplicate independent experiments

As shown in Table 1, the synthesized molecules 1, 3-5 presented concentration-dependent inhibition potency with varying percentages against the α-glucosidase. Structure-activity relationship analysis demonstrated that electron-donating groups (e.g., *p*-methoxy in compound 3) enhance high-concentration potency (26.28% at 0.2 mM), while electron-withdrawing groups (e.g., *p*-carboxy in compound 4 and *p*-nitro in compound 5) confer superior low-to-moderate concentration efficacy, with compound 4 achieving 32.45% inhibition at 0.1 mM and compound 5 showing remarkable low-dose activity (18.01% at 0.025 mM).

Among the synthesized quinoxaline-hydrazone derivatives, compound 2, bearing a *para*-hydroxy substituent on the phenyl ring, emerged as the most potent inhibitor with an IC_{50} value of 0.413 ± 0.048 mM, representing a 2.93-fold enhancement over acarbose (IC_{50}= 1.211 ± 0.08 mM). Therefore, this benzaldehyde hydrazone derivative, which bears electron donor hydroxyl substituent at the *para* position of the phenyl ring seems to have promising inhibitory activity to α-glucosidase enzyme, which is a critical therapeutic target in type 2 diabetes management. Regarding the biological activity data, it can be speculated that designed general structure may produce potent α-glucosidase inhibitors for the treatment of type 2 diabetes.

Enzyme Kinetic Study

To elucidate the mechanism of inhibition of the synthesized compound, *in vitro* enzyme kinetic studies were conducted as described in the Material and Method section. The results demonstrated that increasing inhibitor concentrations maintained similar maximum reaction rates (V_{max}) while increasing the Michaelis constant (K_m). Accordingly, Michaelis-Menten and Lineweaver-Burk plots (Figure 2) showed that the compound functions as a competitive inhibitor of *α*-glucosidase ($r^2 = 0.99$). Competitive inhibitors bind reversibly to the enzyme's active site (Figure 3), increasing the apparent K_m for the substrate without altering V_{max} [25]. Furthermore, secondary plots of K_m versus inhibitor concentration yielded an inhibitory constant (K_i) of 115.6 µM.

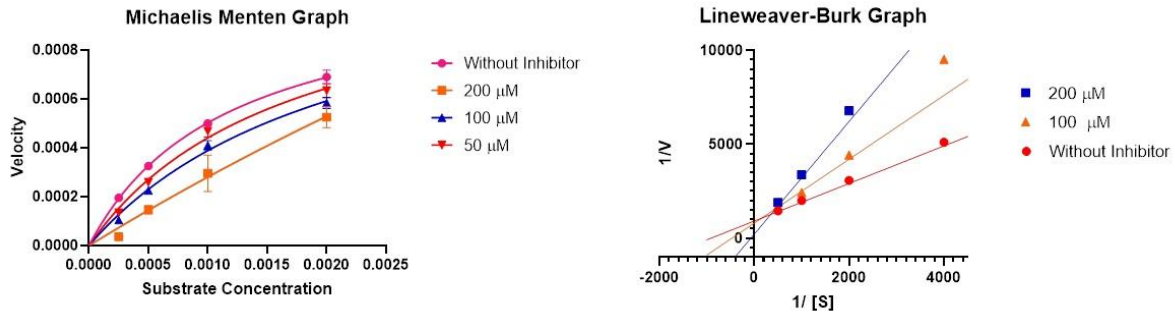

Figure 2. Michaelis-Menten and Lineweaver-Burk graphs of compound 2

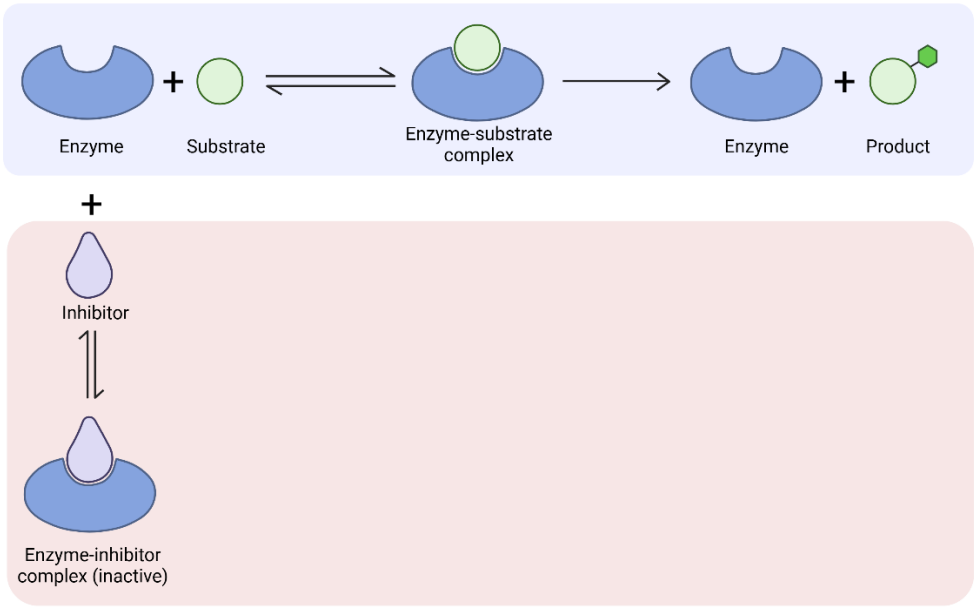

Figure 3. Competitive enzyme inhibition model. Adapted from "Competitive inhibition", by BioRender (2025) [41]

Molecular Docking Study

Molecular docking simulations were conducted to assess the binding interactions, orientation, and affinity of the synthesized compound at the α-glucosidase active site. Consistent with the experimentally determined competitive inhibition mechanism, a competitive docking model was constructed. The docking results demonstrated correlation with the IC_{50} values presented in Table 3. Analysis of binding interactions revealed that compound 2 forms hydrogen bonds with catalytic residues Asp214 (1.69 Å), Arg212, and Asp408, while exhibiting an acidic interaction with Glu276 (Figures 4 and 5). In comparison, the reference inhibitor acarbose forms hydrogen bonds with Arg439 and acidic interactions with Asp214 and Glu276. Collectively, the interaction profiles and binding poses indicate that compound 2 inhibits α-glucosidase by occupying the catalytic site, thereby blocking substrate access and preventing enzymatic hydrolysis.

Table 3. Docking scores of compound 2 and Acarbose against the active site of the *α*-glucosidase enzyme

Ligand	Docking Score	Number of Hydrogen Bonds	The Number of Residues
2	54.2786	3	17
Acarbose	55.8873	4	25
α-D-glucopyranose	35.1001	3	12

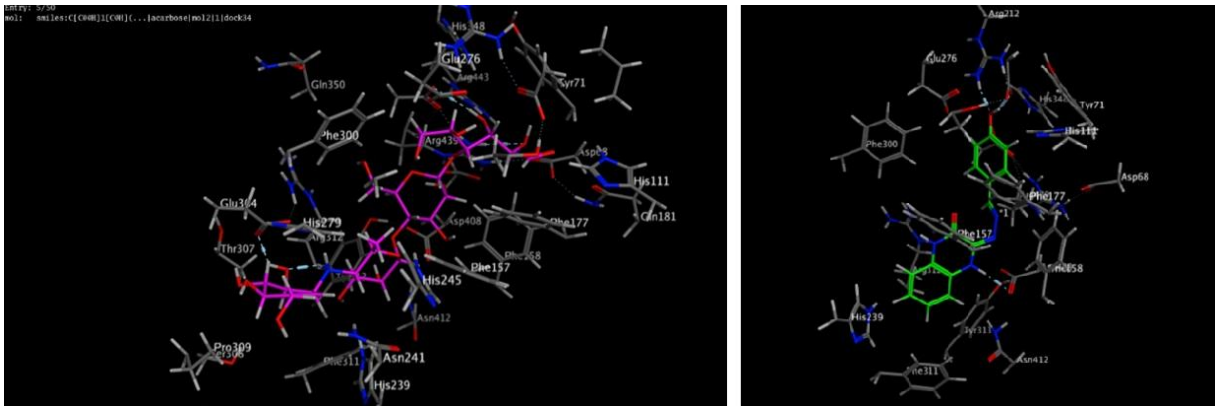

Figure 4. The 3D interaction maps of compound 2 and Acarbose with α-glucosidase active cavity

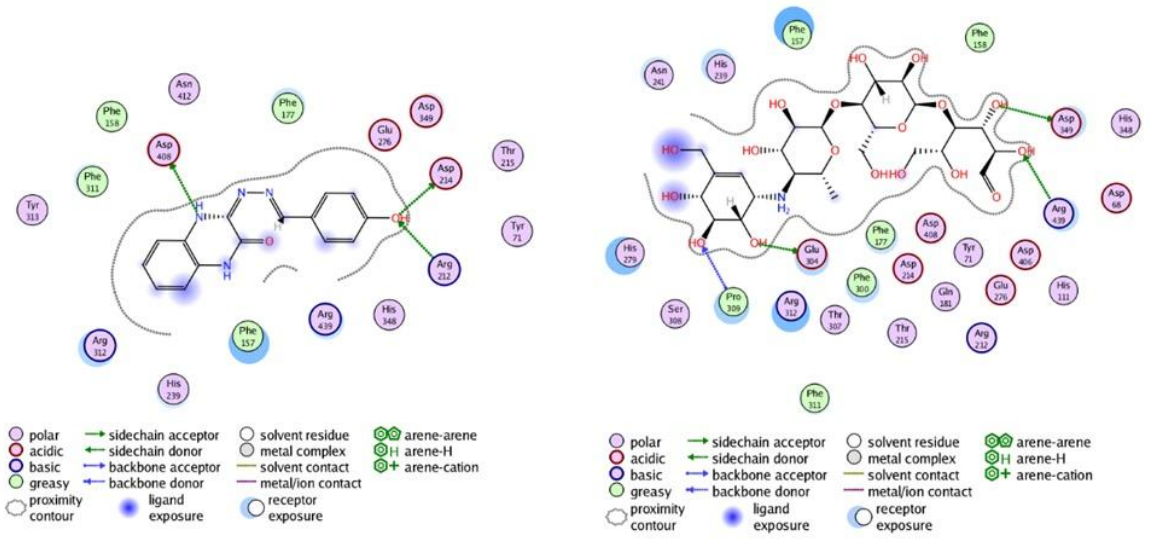

Figure 5. The 2D interaction maps of compound 2 and Acarbose with α-glucosidase active cavity

In conclusion, the synthesized quinoxaline-hydrazone derivatives exhibited concentration-dependent *α*-glucosidase inhibition, with compound 2 bearing a *para*-hydroxy substituent emerging as the most potent inhibitor (IC_{50} = 0.413 ± 0.048 mM), showing 2.93-fold greater activity than acarbose (IC_{50} = 1.211 ± 0.08 mM). Enzyme kinetic studies confirmed compound 2 acts as a competitive inhibitor (K_i = 115.6 µM), with molecular docking revealing key hydrogen bonds between its hydroxyl group and catalytic residues (Asp214, Arg212, Asp408) and an acidic interaction with Glu276. These preliminary findings collectively demonstrate that the quinoxaline-hydrazone scaffold represents a promising structural framework for developing potent α-glucosidase inhibitors as therapeutic agents for diabetes management. Our research will continue to explore this scaffold's therapeutic potential.

ACKNOWLEDGEMENTS

This study was supported by Ege University Scientific Research Project (Grant ID-31974).

AUTHOR CONTRIBUTIONS

Concept: M.A., Z.S.; Design: M.A., Z.S.; Control: M.A., Z.S.; Sources: M.A., Z.S.; Materials: M.A., Z.S.; Data Collection and/or Processing: M.A.; Analysis and/or Interpretation: M.A., Z.S.; Literature Review: M.A., Z.S.; Manuscript Writing: M.A., Z.S.; Critical Review: Z.S.; Other: M.A., Z.S.

CONFLICT OF INTEREST

The authors declare that there is no real, potential, or perceived conflict of interest for this article.

ETHICS COMMITTEE APPROVAL

The authors declare that the ethics committee approval is not required for this study.

REFERENCES

1. Saddique, F.A., Ahmad, M., Ashfaq, U.A., Ahmad, M.N., Anjum, M.N., Mohsin, N.A., Aslam, S. (2019). Alpha-glucosidase inhibition and molecular docking studies of 1,2-benzothiazine 1,1-dioxide based carbohydrazides. Pakistan Journal of Pharmaceutical Sciences, 32, (6(Supplementary)), 2829-2834. [CrossRef]
2. Liu, Z., Ma, S. (2017). Recent advances in synthetic α-glucosidase inhibitors. ChemMedChem, 12(11), 819-829. [CrossRef]
3. Missioui, M., Mortada, S., Guerrab, W., Serdaroğlu, G., Kaya, S., Mague, J.T., Essassi, E.M., Faouzi, M.E.A., Ramli, Y. (2021). Novel antioxidant quinoxaline derivative: Synthesis, crystal structure, theoretical studies, antidiabetic activity and molecular docking study. Journal of Molecular Structure, 1239, 130484. [CrossRef]
4. Dhameja, M., Gupta, P. (2019). Synthetic heterocyclic candidates as promising α-glucosidase inhibitors: An overview. European Journal of Medicinal Chemistry, 176, 343-377. [CrossRef]
5. Israhili, Z.H. (2011). Advances in the treatment of type 2 diabetes mellitus. American Journal of Therapeutics, 18(2), 117-152. [CrossRef]
6. Feng, Y., Nan, H., Zhou, H., Xi, P., Li, B. (2022). Mechanism of inhibition of *α*-glucosidase activity by bavachalcone. Food Science and Technology, 42, e123421. [CrossRef]
7. Hedrington, M.S., Davis, S.N. (2019). Considerations when using *alpha*-glucosidase inhibitors in the treatment of type 2 diabetes. Expert Opinion on Pharmacotherapy, 20(18), 2229-2235. [CrossRef]
8. National Collaborating Centre for Chronic Conditions (UK). Type 2 Diabetes: National Clinical Guideline for Management in Primary and Secondary Care (Update) Web site. (2008). Retrieved August 02, 2025, from https://www.ncbi.nlm.nih.gov/books/NBK53885/. Accessed date: 02.12.2025.
9. Wang, G., Chen, M., Wang, J., Peng, Y., Li, L., Xie, Z., Deng, B., Chen, S., Li, W. (2017). Synthesis, biological evaluation and molecular docking studies of chromone hydrazone derivatives as *α*-glucosidase inhibitors. Bioorganic and Medicinal Chemistry Letters, 27(13), 2957-2961. [CrossRef]
10. Zhang, L., Song, P., Zhang, X., Metea, C., Schleisman, M., Karstens, L., Leung, E., Zhang, J., Xu, Q., Liu, Y., Asquith, M., Chu, C. (2020). *Alpha*-glucosidase inhibitors alter gut microbiota and ameliorate collagen-induced arthritis. Frontiers in Pharmacology, 10, 1684. [CrossRef]
11. Li, X., Bai, Y., Jin, Z., Svensson, B. (2022). Food-derived non-phenolic *α*-amylase and *α*-glucosidase inhibitors for controlling starch digestion rate and guiding diabetes-friendly recipes. Lebensmittel-Wissenschaft & Technologie, 153, 112455. [CrossRef]
12. Jampilek, J. (2019). Heterocycles in medicinal chemistry. Molecules, 24 (21), 3839. [CrossRef]
13. Hameed, S., Khan, K.M., Taslimi, P., Salar, U., Taskin-Tok, T., Kisa, D., Saleem, F., Solangi, M., Ahmed, M.H.U., Rani, K. (2022). Evaluation of synthetic 2-aryl quinoxaline derivatives as *α*-amylase, *α*-glucosidase, acetylcholinesterase, and butyrylcholinesterase inhibitors. International Journal of Biological Macromolecules, 211, 653-668. [CrossRef]

14. Alasmary, F.A., Alnahdi, F.S., Ben Bacha, A., El-Araby, A.M., Moubayed, N., Alafeefy, A.M., El-Araby, M.E. (2017). New quinoxalinone inhibitors targeting secreted phospholipase A2 and α-glucosidase. Journal of Enzyme Inhibition and Medicinal Chemistry, 32(1), 1143-1151. [CrossRef]
15. Scattolin, T., Bouayad-Gervais, S., Schoenebeck, F. (2019). Straightforward access to N-trifluoromethyl amides, carbamates, thiocarbamates and ureas. Nature, 573, 102-107. [CrossRef]
16. Tariq, S., Somakala, K., Amir, M. (2018). Quinoxaline: An insight into the recent pharmacological advances. European Journal of Medicinal Chemistry, 143, 542-557. [CrossRef]
17. Rollas, S., Küçükgüzel, Ş.G. (2007). Biological activities of hydrazone derivatives. Molecules, 12(8), 1910-1939. [CrossRef]
18. de Oliveira Carneiro Brum J., França T.C.C., LaPlante S.R., Villar J.D.F. (2020). Synthesis and biological activity of hydrazones and derivatives: A review. Mini-Reviews in Medicinal Chemistry, 20(5), 342-368. [CrossRef]
19. Bouanane, Z., Bounekhel, M., Elkollı, M., Takfaou, A. (2011). A new solvent for the reaction of chlorination of hydroxyquinoxaline derivatives with Vilsmeier reagent. Archives of Applied Science Research, 3(1), 380-391.
20. Ajani, O.O., Obafemi, C.A., Ikpo, C.O., Ogunniran, K.O., Nwinyi, O.C. (2009). Microwave-assisted synthesis and antibacterial activity of some pyrazol-1-ylquinoxalin- 2(1*H*)-one derivatives. Chemistry of Heterocyclic Compounds, 45(11), 1370-1378. [CrossRef]
21. Galal, S.A., Abdelsamie, A.S., Soliman, S.M., Mortier, J., Wolber, G., Ali, M.M., Tokuda, H., Suzuki, N., Lida, A., Ramadan, R.A., El Diwani, H.I. (2013). Design, synthesis and structure-activity relationship of novel quinoxaline derivatives as cancer chemopreventive agent by inhibition of tyrosine kinase receptor. European Journal of Medicinal Chemistry, 69, 115-124. [CrossRef]
22. Hesse, M., Meier, H., Zeeh, B. (1997). Spectroscopic Methods in Organic Chemistry, Georg Thieme Verlag, Stuttgart-New York, p.202-356. [CrossRef]
23. Silverstein, R.M., Webster, F.X., Kiemle, D.J. (2005). Spectrometric Identification of Organic Compounds, 7th Edition, John Wiley & Sons, Inc., Hoboken, p.144-249.
24. El Hamid, M.K., Mihovilovic, M.D., El-Nassan H.B. (2012). Synthesis of novel pyrazolo[3,4-*d*] pyrimidine derivatives as potential anti-breast cancer agents. European Journal of Medicinal Chemistry, 57, 323-328. [CrossRef]
25. Pelley, J.W. (2012). Enzyme and Energetics. Elsevier's Integrated Review Biochemistry, Philadelphia, p.29-37. [CrossRef]
26. Ayan, E.K., Soyer, Z., Uysal, S. (2021). Synthesis and enzymological characterization of some 2-(substitutedphenylamino)quinazolin-4(3*H*)-one derivatives as potent α-glucosidase inhibitors *in vitro*. Letters in Drug Design and Discovery, 18, 723-732. [CrossRef]
27. Ranilla, L.G., Kwon, Y.I., Apostolidis, E., Shetty, K. (2010). Phenolic compounds, antioxidant activity and in vitro inhibitory potential against key enzymes relevant for hyperglycemia and hypertension of commonly used medicinal plants, herbs and spices in Latin America. Bioresource Technology, 101(12), 4676-4689. [CrossRef]
28. Uniprot Website. (2025). Retrieved June 18, 2025 from https://www.uniprot.org/uniprot/P53341. Accessed date: 02.12.2025.
29. The UniProt Consortium. (2015). UniProt: a hub for protein information, Nucleic Acids Research, 43 (D1), D204–D212. [CrossRef]
30. Pettersen, E.F., Goddard, T.D., Huang, C.C., Couch, G.S., Greenblatt, D.M., Meng, E.C., Ferrin, T.E. (2004). UCSF Chimera-A visualization system for exploratory research and analysis. Journal of Computational Chemistry, 25, 1605-1612. [CrossRef]
31. Colovos, C., Yeates, T.O. (1993). Verification of protein structures: Patterns of nonbonded atomic interactions. Protein Science, 2(9), 1511-1519. [CrossRef]
32. Bowie, J.U., Lüthy, R., Eisenberg, D. (1991). A method to identify protein sequences that fold into a known three-dimensional structure. Science, 253(5016), 164-170. [CrossRef]
33. Laskowski, R.A., MacArthur, M.W., Moss, D.S., Thornton, J.M. (1993). PROCHECK-a program to check the stereochemical quality of protein structures. Journal of Applied Crystallography, 26, 283-291. [CrossRef]
34. Sumran, G., Aggarwal, R., Mittal, A., Aggarwal, A., Gupta, A. (2019). Design, synthesis and photoinduced DNA cleavage studies of [1,2,4]-triazolo[4,3-*a*]quinoxalin-4(5*H*)-ones. Bioorganic Chemistry, 88, 102932. [CrossRef]
35. Galal, S.A., Abdelsamie, A.S., Tokuda, H., Suzuki, N., Lida, A., El Hefnawi, M.M., Ramadan, R.A., Atta, M.H.E., El Diwani, H.I. (2011). Part I: Synthesis, cancer chemopreventive activity and molecular docking

study of novel quinoxaline derivatives. European Journal of Medicinal Chemistry, 46(1), 327-340. [CrossRef]

36. Kshirsagar, S.S., Nimje, H.M., Chaudhari, P.S., Bayas, J.P., Patel, E.K., Karjikar, A.H., Girme, P.D., Oswal, R.J. (2011). Synthesis and antimicrobial activity of novel thiazolidinone and azetidinone derivatives. Asian Journal of Chemistry, 23(9), 4021-4023.
37. Ajani, O.O., Nwinyi, O. (2009). Synthesis and evaluation of antimicrobial activity of phenyl and furan-2-yl[1,2,4] triazolo[4,3-*a*]quinoxalin-4(5*H*)-one and their hydrazone precursors. Canadian Journal of Pure and Applied Sciences, 3(3), 983-992.
38. Bayoumi, A.H., Ghiaty, A.H., Abd El-Gilil, S.M., Husseiny, A.M., Ebrahim, M.A. (2019). Exploration of quinoxaline derivatives as antimicrobial and anticancer agents. Journal of Heterocyclic Chemistry, 56(12), 3215-3235. [CrossRef]
39. Rashed, N., El Massry, A.M., El Ashry, E.S.H., Amer, A., Zimmer, H. (1990). A facile synthesis of novel triazoloquinoxalinones and triazinoquinoxalinones. Journal of Heterocyclic Chemistry, 27(3), 471-822. [CrossRef]
40. El-Sayed, N.N.E., Al-Otaibi, T.M., Alonazi, M., Masand, V.H., Barakat, A., Almarhoon, Z.M., Abir, B.B. (2021). Synthesis and characterization of some new quinoxalin-2(1*H*)one and 2-methyl-3*H*-quinazolin-4-one derivatives targeting the onset and progression of CRC with SAR, molecular docking, and ADMET analyses. Molecules, 26(11), 3121. [CrossRef]
41. Biorender Website. (2025). Retrieved July 28, 2025, from https://app.biorender.com/biorender-templates/. Accessed date: 02.12.2025.